Granular flow from silos with rotating orifice

Kiwing To,[1,*] Yun Yen,[1,2] Yi-Kai Mo,[1] and Jung-Ren Huang[1]
[1]*Institute of Physics, Academia Sinica, Taipei, Taiwan, Republic of China*
[2]*Department of Physics, National Taiwan University, Taipei, Taiwan, Republic of China*

(Received 1 February 2019; revised manuscript received 30 May 2019; published 18 July 2019)

For dry granular materials falling through a circular exit at the bottom of a silo, no continuous flow can be sustained when the diameter D of the exit is less than five times the characteristic size of the grains. If the bottom of the silo rotates horizontally with respect to the wall of the silo, finite flow rate can be sustained even at small D. We investigate the effect of bottom rotation to the flow rate of monodisperse plastic beads of $d = 6$ mm diameter from a cylindrical silo of 19 cm inner diameter. We find that the flow rate W follows Beverloo law down to $D = 1.3d$ and that W increases with the rotation speed ω in the small exit regime. If the exit is at an off-center distance R from the axis of the silo, W increases with the rate of area swept by the exit. On the other hand, when the exit diameter is large, W decreases with increasing ω at small ω but increases with ω at large ω. Such nonmonotonic dependence of flow rate on rotation speed may be explained as a gradual change from funnel flow to mass flow due to the shear at the bottom of the silo.

DOI: 10.1103/PhysRevE.100.012906

I. INTRODUCTION

Discharge of dry granular materials from hoppers and silos is a process which has been studied for a long time. Intuitively, the outflow rate of grains from silos and hoppers increases with the size of the orifice. The empirical observation between flow rate W and orifice size D: $W \propto (D - D_o)^{5/2}$ by Beverloo *et al.* [1] has been confirmed when D is much larger than the characteristic size of the grains. Other factors, such as friction [2,3], elasticity, and shape of the grains [4–6], hopper geometry [7,8], external perturbations [9,10], interstitial fluid [11,12],..., etc., have, in general, only a minor effect on flow rate except in silos of small orifice sizes. In practice, Beverloo law breaks down for small exit size when the flow is clogged stochastically [3,13,14]. The experimentally observed clogging transition probability can be fitted equally well to either an exponential decaying function or an algebraic function [15–18].

These results led to a fundamental question of the existence of the no-clog regime when the exit size is larger than a critical value. In contrast, unclogging transition may involve collective rearrangement of the grains [19] in the packing with a much larger length scale than exit size. Despite a large amount of experimental, theoretical, and computational studies in clogging and unclogging in granular flow through bottlenecks, quantitative theories that successfully explain these two stochastic transitions are yet to be found.

Since hoppers and silos are very common industrial and agricultural appliances that are used as transporting or distributing granular materials, there are devices (vibrator, air cannons, etc.) invented to prevent clogging and keep the material flowing continuously. Recently, it was found that a small motion of the exit effectively avoids clogging in the small exit regime [20].

However, the effect of exit motion to flow rate is not clearly understood yet. It has been known that clogging is due to formation of an arch in two-dimensional silos (or a dome in three-dimensional silos) at the exit that blocks the flow [3,4,13,14]. Hence, to prevent clogging, it is crucial to prevent formation of the arch and/or break the arch once it is formed. As demonstrated by To and Tai [20], an efficient way is to let go of the bases of the arch that blocks the flow in a two-dimensional silo by moving the exit beneath them. However, the motion of the exit not only destroys the arch by going under the bases of the arch, but also shears the materials in the two-dimensional silo.

In order to study the effect of shear at the bottom on the granular flow through a silo, we constructed a three-dimensional silo with a rotatable bottom. When the circular exit is at the center of the bottom of the silo, rotating the bottom shears the material in the silo whereas the exit remains stationary. We find that, at small exit sizes, rotation of the bottom increases the flow rate as expected from a simple physical argument and observed by numerical simulations [10,21]. Surprisingly, when the exit size is large, rotation of the bottom reduces the flow rate at small rotation speed but increases the flow rate at large rotation speed. We observe that the nonmonotonic dependence of flow rate on rotation speed may be related to a change in the flow pattern—from funnel flow to mass flow in the silo.

In the rest of the paper, we will give an account of the experimental setup and procedures. Then, the measurement of flow rate at different sizes, positions, and rotation speeds of the exit will be presented along with our understanding of the observed behavior. Afterward, we will discuss possible physical pictures that may lead to the observed minimum in flow rate due to rotation of the exit of the silo.

*ericto@gate.sinica.edu.tw

II. EXPERIMENTAL METHODS

A schematic and a photograph of the experimental setup are shown in Fig. 1. A transparent acrylic cylindrical silo of 19 cm diameter is securely mounted on an aluminum frame. The bottom of the silo can rotate about the axis of the silo with respect to the stationary cylindrical wall. The rotation speed can be controlled from 0.08 revolutions per second (rps) to 1.0 rps by a DC motor (Oriental Motor BLFD30A2) through a belt pulley mechanism. The exit from the silo is a circular orifice of diameter D at a distance R from the center of the silo. At the beginning of an experiment, 8 kg (about 3×10^4) of plastic beads (diameter 6 mm and mass 0.27 g) are loaded into the silo with the exit blocked. The bottom of the silo is set to rotate at the designated speed ω before the exit is unblocked. The beads fall from the silo through the exit into the collecting bin whose weight is monitored every 0.1 s by an electronic balance (Satorius CP-34001P) which is configured to output only the mass of the beads in the bin to a personal computer (Asus Eee BOX B202).

Figure 2 shows the time variation of the reading m from the electronic balance for four different sets of the three control parameters: exit diameter D, off-center distance R, and rotation speed ω. One can see that the total mass of the beads discharged from the silo increases linearly with time until the silo is almost empty. From these data, it is easy to find that the flow rate increases with increasing D, R, as well as ω. A quantitative measurement of the flow rate is obtained by linear regression using the data in the early stage of discharge when $m < 2000$ g. In most cases, five measurements of the flow rate is conducted for each set of the experimental condition. The mean value of these measurements is reported as W, and the standard deviation is taken as the uncertainty in W.

Figure 3 shows the variation of flow rate W with respect to exit diameter D when the exit is at the center of the silo (i.e., $R = 0$) and the rotation speed set at $\omega = 1/6$ rps. The nonlinear growth of W with D can be fitted to the Beverloo law $W \propto (D - D_o)^{5/2}$ as illustrated by the inset in which the data fall on a straight line when $W^{0.4}$ is plotted against D.

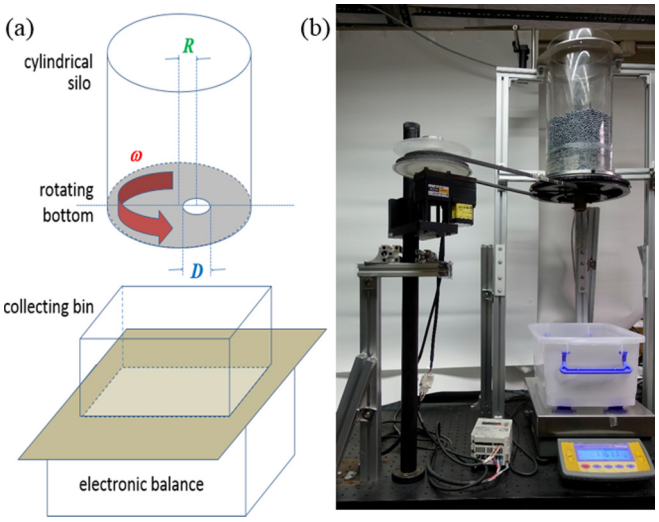

FIG. 1. (a) Schematic of the experimental setup. (b) Photograph of the actual experimental setup.

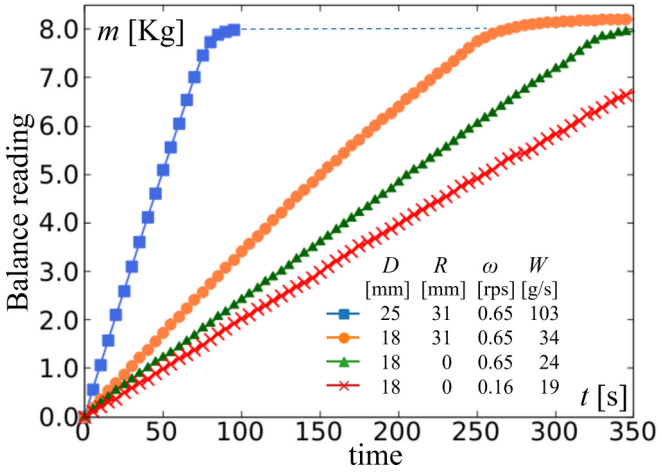

FIG. 2. Time records of the reading m from the electronic balance during discharge at different control parameters (D, R, and ω) and the flow rates W obtained from linear regression using data $m < 2$ kg.

Hence, Beverloo law is valid for the silo with the rotating bottom. It should be pointed out that, if the bottom does not rotate (i.e., $\omega = 0$), continuous flow cannot sustain (i.e., W vanishes) for $D \lessapprox 30$ mm. This implies that bottom rotation extends the validity of the Beverloo law down to $D = 7.8$ mm which is only 1.3 time the diameter of the bead. This finding is consistent to those obtained by Thomas and Durian [22] and Mankoc and co-workers [23,24]. In their works, the silo exit did not move, and the flow rate in the clogging regime was taken as the mean value of the ratio of the weight of the grains discharged before clogging divided by the duration of flow in repeated flow and clog events.

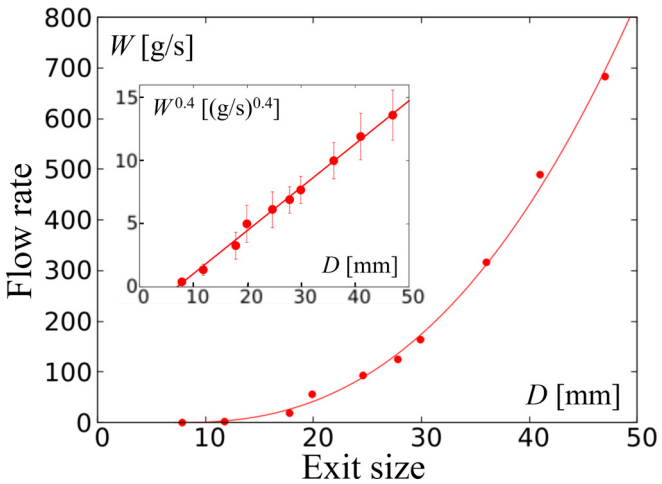

FIG. 3. Flow rate W versus exit diameter D for $R = 0$ and $\omega = 1/6$ rps. The uncertainty in W is smaller than the size of the symbols. The inset: The same data plotted in $W^{0.4}$ versus D. Lines in this graph and the inset are the fitted curves of the data to Beverloo law $W = 0.069(D - 6.96)^{5/2}$.

III. RESULTS AND DISCUSSIONS

To investigate the effect of bottom rotation and exit position on flow rate, we measure the flow rate W when the center of the exit is set to a distance R from the center of the silo. The results for exit diameter of $D = 7.8$ mm are shown in Fig. 4. Although W increases with ω as expected, the enhancement of flow rate by exit rotation is more effective when the exit is farther away from the center of the silo. If we compare the flow rate at $R = 40$ mm to that at the center (i.e., $R = 0$ mm), an increase by a factor of 10 in W is found. Although W increases with R and ω in a nontrivial way, it may be understood by a simple arch breaking mechanism similar to that proposed in Ref. [20]. When the exit is small, arches that block the flow will form readily after the previous arch is broken when the exit passes under the bases of the arch. For each arch breaking event, a certain number of beads, which should be proportional to the area of the exit, will be discharged. Since the arch breaking rate should increase with the rotation speed of the exit, it is reasonable that the flow rate should also increase with the area swept by the exit per unit time. The region swept by the exit in one complete revolution is an annulus (see the schematic in Fig. 5) of area $\pi[(R + D/2)^2 - (R - D/2)^2] = 2\pi RD$ if $R > D/2$ or a circle of area $\pi(R + D/2)^2$ if $R \leqslant D/2$. Hence, the area sweep rate of the exit is $A = 2\pi RD\omega$ for $R > D/2$ or $\pi(R + D/2)^2\omega$ otherwise. Thus, the flow rate should depend only on the area sweep rate so that W should collapse on a single curve when plotted against A.

When the data in Fig. 4 are plotted against the area sweep rate, they indeed fall on a single curve which can be fitted to a power law with an exponent of 0.68 (see Fig. 5). Note that the argument of letting go of the bases of the arch that block the flow due to exit motion would suggest an exponent of 1.00. Clearly, there are cases when the arch is broken not at the bases but at some other parts of the arch. If the rate of arch breaking due to this mechanism (arch breaking not at the bases) is independent of the rotation speed, the exponent should be less than unity.

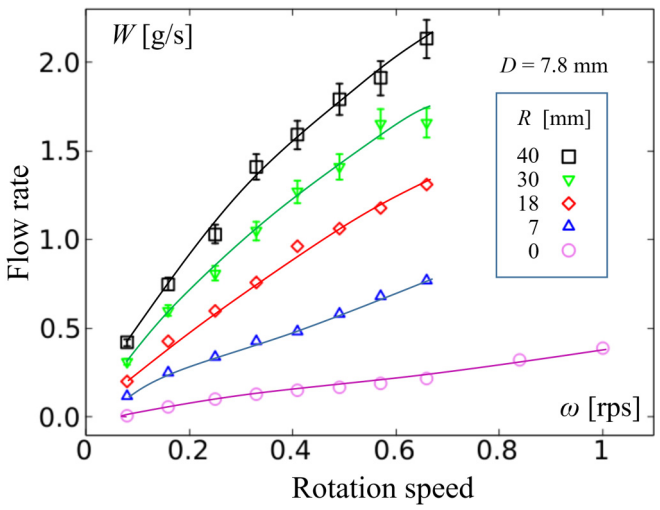

FIG. 4. Graph of flow rate W versus rotation speed ω at different off-center distance R for silo with exit diameter $D = 7.8$ mm. Error bars are smaller than the symbols for $R < 30$ mm, and lines in the graph are guides for the eyes only.

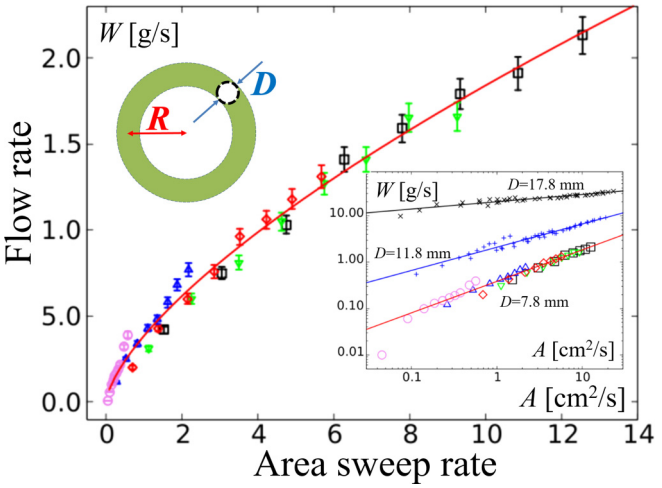

FIG. 5. Flow rate W versus area sweep rate A (the same data as in Fig. 4) for exit diameter $D = 7.8$ mm. The red line through the data is a fitted curve: $W = 0.38A^{0.68}$. The inset: log-log plot of W versus A for exit diameter $D = 7.8$, 11.8 (+), and 17.8 mm (×). The blue line through the + is a fitted curve: $W = 2.1A^{0.5}$ and the black line through the × is $W = 20A^{0.16}$. The top-left schematic shows the region swept by the exit in one complete revolution when $R > D/2$.

Moreover, in the time intervals between the formation of arches, the beads flow continuously with a flow rate that is insensitive to the rotation speed, i.e., $W \propto A^0$. Since the contributions to the flow rate from these two mechanisms increase with increasing exit diameter, the exponent should be smaller in silos of larger exit diameter. Indeed, the fitted exponent for larger exit diameters decreases to 0.5 and 0.16, respectively, for $D = 11.8$ and 17.8 mm as shown in the inset of Fig. 5. Since the exponent indicates how strongly the flow rate depends on rotation speed, one can conclude that the influence of rotation speed on the flow rate decreases with increasing exit diameter.

This trend can be seen by plotting the normalized flow rate $W_n(\omega) \equiv W(\omega)/W(1)$ in Fig. 6. Here, the notation $W(\omega)$ is used to emphasize the explicit dependence of flow rate W on rotation speed ω. In this graph, the flow rate data fall into two groups: small exit ($D = 18$ mm) of strong dependence on ω and large exit ($D = 19$ mm) of weak dependence on ω. To compare quantitatively how flow rate is affected by exit rotation, we calculate the normalized flow rate difference $\Delta W_n \equiv W_n(0.16) - W_n(0.08)$ which is an approximation to the rate of change in flow rate with respect to rotation speed at small ω.

We find that ΔW_n decreases with exit size and turns negative when $D > 25$ mm. Hence, exit rotation enhances flow rate for small exit sizes but reduces flow rate when exit size is larger than a critical value of $D_c \approx 25$ mm. In other words, exit rotation which prevents clogging, has no effect on flow rate when $D = D_c$. Therefore, one may interpret this critical value as the transition between clogging and continuous flow.

Note that the critical value of $D_c \approx 25$ mm is about 4.2 times the diameter of the beads which is smaller than the critical exit diameter (normalized by the grain diameter) of

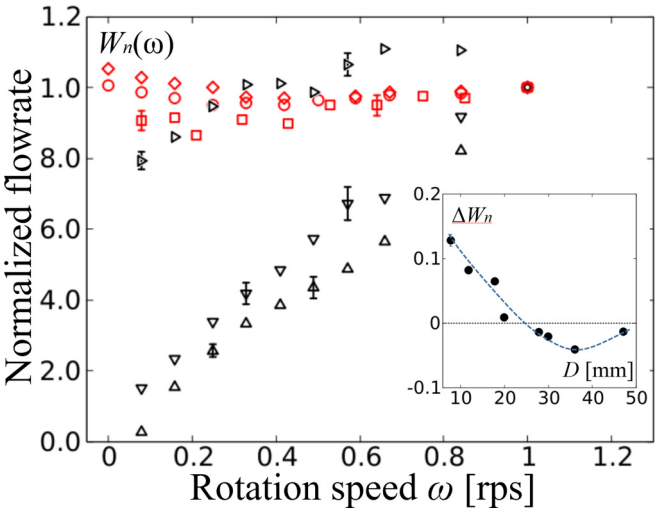

FIG. 6. Normalized flow rate $W_n(\omega)$ versus rotation speed ω when $R = 0$ and $D = 7.8$ mm (△), 11.8 mm (▽), 17.8 mm (▷), 19.9 mm (□), 29.9 mm (◯), and 36.0 mm (◊). For clarity, only a few error bars are plotted for △, ▽, ▷, and □. Error bars for ◯ and ◊ are smaller than the symbols. The inset: Normalized flow rate difference ΔW_n for different exit diameters. The line in the inset is a guide for the eyes only.

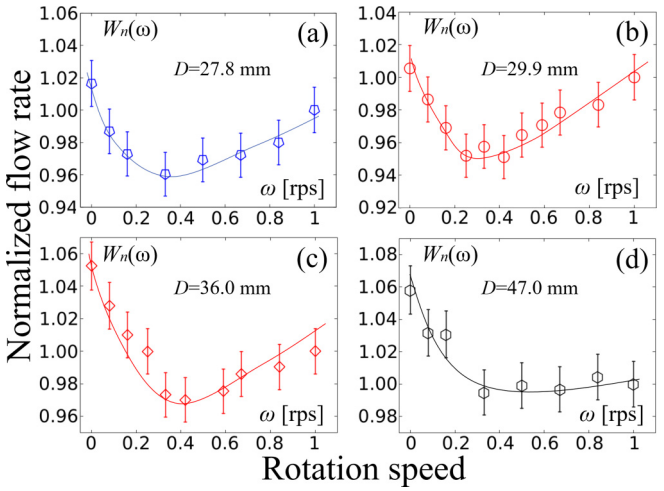

FIG. 7. Normalized flow rate $W_n(\omega)$ versus rotation speed ω for the silo with an exit at the center (i.e., $R = 0$ mm) and (a) diameter $D = 27.8$ mm, (b) 29.9 mm, (c) 36.0 mm, and (d) 47.0 mm. The lines in the graphs are guide for the eyes only.

clogging transition in silos with stationary exit [14,22]. The reduction of the critical exit size had been reported in simultaneous discharge of a mixture of liquid and grains [11,12] in which fluidization was believed to be the cause. In our experiments with dry grains, the smaller critical exit size may be a result of the fluidization of the beads induced by the motion of the bottom of the silo.

Although the flow rate enhancement at small exit sizes has been explained in previous paragraphs, the physics underlying the reduction of flow rate at large exit sizes is not clear. The explanation given in Ref. [20] for the two-dimensional silo with an oscillating exit cannot apply to our three-dimensional silo with a rotating exit at the center of the silo because the rotation of the exit does not involve motion of the edge of the exit in the radial direction. A closer look at the flow rate for large exit sizes leads to the discovery of a minimum in $W_n(\omega)$ at $\omega = \omega_c \approx 0.4$ rps as illustrated in Fig. 7.

The presence of a minimum in $W_n(\omega)$ implies a qualitative change in the discharge process from flow reduction for low rotation speed to flow enhancement for high rotation speed. Such a change seems to be related to a crossover from funnel flow to mass flow as observed from the shape of the top surface of the grains in the silo. When the exit is stationary, we observe a depression at the center of the top surface as shown by a light sheet generated from the beam of a laser pointer through a glass rod [see Fig. 8(a)]. This is a typical feature of funnel flow [25] such that an active flow (blue) region forms above the exit with a stagnant zone at the periphery as shown schematically by the gray region in Fig. 8(b). In contrast, when the bottom is rotating, the top surface is flat, and depression is observed at the wall of the silo as shown in Fig. 8(c). In fact, beads at the wall of the silo near the bottom are not stationary but move downward and then move inward when they reach the bottom. Hence, flow along the wall and the bottom of the silo exists during the discharge as shown schematically in Fig. 8(d). When this current [red arrows in Fig. 8(d)] arrives at the exit, its direction is perpendicular to that of the current (black arrows) along the central part of the silo. Collisions between the beads in these two currents will generate upward impulses that reduce the overall flow rate similar to that observed in the two-dimensional silo with the oscillation exit [20]. As the rotation speed increases, the flow along the bottom increases, and the outflow rate reduction increases. The stagnation region should also shrink with increasing rotation speed. Presumably, before the stagnation

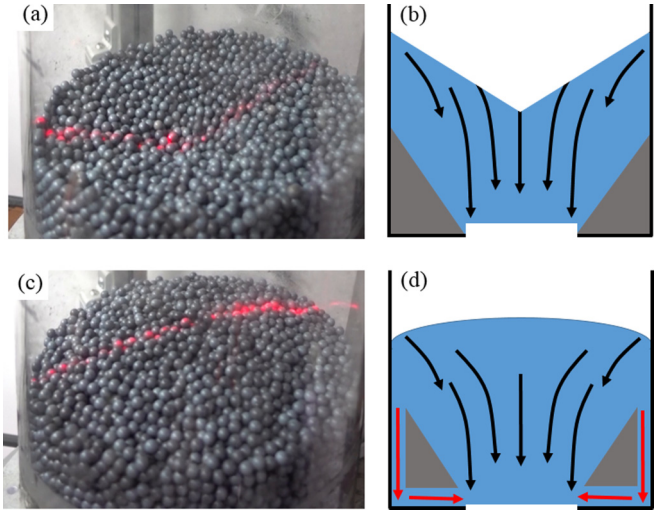

FIG. 8. The shape of the top layer of the bead packing in the discharging silo with exit diameter $D = 41$ mm and the schematic of the possible flow patterns inside the silo for [(a) and (b)] $R = 0$ mm, $\omega = 0$ rps, and [(c) and (d)] $R = 0$ mm, $\omega = 1$ rps. The black arrows in (b) and (d) represent the direction of the motion of the beads through the central region of the silo whereas the red arrows in (d) represent the flow of the beads along the wall and the bottom of the silo.

region vanishes as the rotation speed reaches ω_c, the crossover from funnel flow to mass flow is complete. A further increase in ω leads to a higher degree of fluidization and higher flow rate.

IV. SUMMARY

To summarize, we report experimental results on granular flow through a circular orifice in a silo with a rotating bottom. We find that exit rotation prevents permanent clogging at small exit diameters, and the Beverloo law, which relates the flow rate to the exit diameter D, is found to be valid for D down to 1.3 times the diameter of the grains. In a silo with a rotating bottom and orifice at a distance from the center of the silo, flow rate increases not only with the exit diameter, but also with the area swept by the exit per unit time. Surprisingly, when the exit diameter is large, the flow rate goes through a minimum as the rotation speed increases.

The nonmonotonic variation of flow rate with rotation speed can be explained by a change from funnel flow to mass flow as evident from the shape of the top surface of the grain packing in the silo. Preliminary results [26,27] from numerical simulations using the discrete element method agree qualitatively to the change in flow pattern due to bottom rotation. Details of the numerical simulations will be reported in the future.

ACKNOWLEDGMENTS

The authors would like to thank Dr. T. Börzsönyi, Professor R. Cruz Hidalgo, and T. Pongo for valuable discussions and constructive comments. This research was supported by the Ministry of Science and Technology of the Republic of China Grant No. MOST-107-2112-M-001-025.

[1] W. A. Beverloo, H. A. Leniger, and J. van de Velde, Chem. Eng. Sci. **15**, 260 (1961).
[2] A. Ashour, T. Trittel, T. Börzsönyi, and R. Stannarius, Phys. Rev. Fluids **2**, 123302 (2017).
[3] L. Pournin, M. Ramaioli, P. Folly, and T. M. Liebling, Eur. Phys. J. E **23**, 229 (2007).
[4] A. Ashour, S. Wegner, T. Trittel, T. Borzsonyi, and R. Stannarius, Soft Matter **13**, 402 (2017).
[5] X. Hong, M. Kohne, M. Morrell, H. R. Wang, and E. R. Weeks, Phys. Rev. E **96**, 062605 (2017).
[6] J. Y. Tang and R. P. Behringer, Europhys. Lett. **114**, 34002 (2016).
[7] R. M. Nedderman, U. Tüzün, S. B. Savage, and G. T. Houlsby, Chem. Eng. Sci. **37**, 1597 (1982).
[8] D. Lopez-Rodriguez, D. Gella, K. To, D. Maza, A. Garcimartin, and I. Zuriguel, Phys. Rev. E **99**, 032901 (2019).
[9] K. To, Chin. J. Phys. **40**, 327 (2002).
[10] E. I. Corwin, Phys. Rev. E **77**, 031308 (2008).
[11] J. Koivisto and D. J. Durian, Nat. Commun. **8**, 15551 (2017).
[12] A. M. Cervantes-Álvarez, S. Hidalgo-Caballero, and F. Pacheco-Vázquez, Phys. Fluids **30**, 043302 (2018).
[13] K. To, P.-Y. Lai, and H. K. Pak, Phys. Rev. Lett. **86**, 71 (2001).
[14] I. Zuriguel, L. A. Pugnaloni, A. Garcimartin, and D. Maza, Phys. Rev. E **68**, 030301(R) (2003).
[15] I. Zuriguel, A. Garcimartin, D. Maza, L. A. Pugnaloni, and J. M. Pastor, Phys. Rev. E **71**, 051303 (2005).
[16] K. To, Phys. Rev. E **71**, 060301(R) (2005).
[17] A. Janda, I. Zuriguel, A. Garcimartín, L. A. Pugnaloni, and D. Maza, Europhys. Lett. **84**, 44002 (2008).
[18] C. C. Thomas and D. J. Durian, Phys. Rev. Lett. **114**, 178001 (2015).
[19] C. Merrigan, S. K. Birwa, S. Tewari, and B. Chakraborty, Phys. Rev. E **97**, 040901(R) (2018).
[20] K. To and H.-T. Tai, Phys. Rev. E **96**, 032906 (2017).
[21] J. Hilton and P. Cleary, Phys. Fluids **22**, 071701 (2010).
[22] C. C. Thomas and D. J. Durian, Phys. Rev. E **87**, 052201 (2013).
[23] C. Mankoc, A. Janda, R. Arévalo, J. M. Pastor, I. Zuriguel, A. Garcimartín, and D. Maza, Granular Matter **9**, 407 (2007).
[24] C. Mankoc, A. Garcimartin, I. Zuriguel, D. Maza, and L. A. Pugnaloni, Phys. Rev. E **80**, 011309 (2009).
[25] F. Pacheco-Vázquez, A. Y. Ramos-Reyes, and S. Hidalgo-Caballero, Phys. Rev. E **96**, 022901 (2017).
[26] T. Pongo (private communication).
[27] C. R. Hidalgo (private communication).